

JOURNAL OF THE STRUCTURAL DIVISION

NONLINEAR FINITE ELEMENT ANALYSIS OF PULL-OUT TEST

By Niels Saabye Ottosen¹

INTRODUCTION

A considerable interest is directed towards determining in-situ concrete properties, and various destructive as well as nondestructive methods are currently applied. Knowledge of the in-situ concrete compressive strength is of particular importance and pull-out tests have been proposed quite early for this purpose (14,15). Newer investigations within this field have been reported, e.g., by Malhotra (9), Clifton (1), and Mailhot, et al. (8). The importance of those pull-out tests, in which a circular steel disc is extracted from the structure using a cylindrical counter pressure, has manifested itself as a tentative standard, i.e., *ASTM-C900-78T*.

The present paper is devoted to nonlinear finite element analysis of such a pull-out test, namely the so-called Lok-Test proposed by Kierkegaard-Hansen (5). The aim of the analysis is to attain a clear insight into the structural behavior. The AXIPLANE program (13) is used for this purpose. In addition to the cracking of the concrete, this program considers the strain hardening and softening in the pre- and post-failure regions, respectively. The influence on the structural behavior of the uniaxial compressive strength, the ratio of tensile to compressive strength, different failure criteria, and post-failure behaviors are investigated. Moreover, because much dispute has been placed on the type of failure actually occurring in the concrete, special attention is given to the structural behavior and the failure mode. Finally, the predictions are compared with published experimental and theoretical results.

¹Research Engr., Risø National Lab., Engrg. Dept., Postbox 49, DK-4000, Roskilde, Denmark.

Note.—Discussion open until September 1, 1981. To extend the closing date one month, a written request must be filed with the Manager of Technical and Professional Publications, ASCE. Manuscript was submitted for review for possible publication on April 3, 1980. This paper is part of the Journal of the Structural Division, Proceedings of the American Society of Civil Engineers, ©ASCE, Vol. 107, No. ST4, April, 1981. ISSN 0044-8001/81/0004-0591/\$01.00.

16197 ANALYSIS OF PULL-OUT TEST

KEY WORDS: Biaxial stresses; Compression tests; Compressive strength; Concretes; Cracking; Failure (mechanics); Finite element method; Materials tests; Mathematical models; Matrix methods; Mechanical properties; Pull-out tests; Softening; Strain hardening; Strength; Stresses; Structural analysis; Triaxial stresses

ABSTRACT: A specific pull-out test used to determine in-situ concrete compressive strength is analyzed. This test consists of a steel disc that is extracted from the structure. The finite element analysis considers cracking, as well as strain hardening and softening in the pre- and post-failure region, respectively. The aim is to attain a clear insight into structural behavior. Special attention is given to the failure mode. Severe cracking occurs and the stress distribution is very inhomogeneous. However, large compressive forces run from the disc in a rather narrow band towards the support and this constitutes the load-carrying mechanism. The failure is caused by the crushing of the concrete in this region, and not by cracking.

REFERENCE: Ottosen, Niels Saabye, "Nonlinear Finite Element Analysis of Pull-Out Test," *Journal of the Structural Division*, ASCE, Vol. 107, No. ST4, Proc. Paper 16197, April, 1981, pp. 591-603

The finite element program AXIPLANE described by the writer (13), and applicable for axisymmetric and plane structures, is applied. Only axisymmetric triangular elements with linear displacement functions are utilized in the present analysis.

In the numerical performance, the total load is considered, even though it is increased stepwise. However, for each load level, iterations are carried out until the constitutive equations for the concrete are in accordance with the total loading in question. To consider the effect of stress redistribution, small load increments, around 2%–4% of the ultimate load, are employed. The failure load is determined as that load in which a large number of iterations—i.e., 25—is insufficient to satisfy both the constitutive equations and the static equilibrium.

The constitution model of the concrete is quite simple to work with and is based on nonlinear elasticity, where the secant values of Young's modulus and Poisson's ratio are changed appropriately (11). This alternation is obtained through use of a nonlinearity index that relates the actual stress state to the failure surface.

Let σ_1 , σ_2 , and σ_3 denote the principal stresses, and let $\sigma_1 \geq \sigma_2 \geq \sigma_3$, in which tensile stress is considered positive; then if only compressive stresses are present, the nonlinearity index, β , is defined as

$$\beta = \frac{\sigma_3}{\sigma_{3f}} \dots \dots \dots (1)$$

in which σ_3 = the actual, most compressive principal stress; and σ_{3f} = the corresponding failure value, provided that the other principal stresses, σ_1 and σ_2 , are unchanged. Thus, $0 \leq \beta < 1$, and $\beta > 1$ correspond to stress states located inside, on, and outside the failure surface, respectively. The nonlinearity index, given by Eq. 1, is proportional to the stress for uniaxial compressive loading, and it can therefore be considered an effective stress. When tensile stresses are present, we transform the actual stress state ($\sigma_1, \sigma_2, \sigma_3$), in which at least σ_1 = a tensile stress, by superposing the hydrostatic pressure, $-\sigma_1$, and obtaining the new stress state ($\sigma'_1, \sigma'_2, \sigma'_3$) = $(0, \sigma_2 - \sigma_1, \sigma_3 - \sigma_1)$, i.e., a biaxial compressive stress state. We then define β as

$$\beta = \frac{\sigma'_3}{\sigma'_{3f}} \dots \dots \dots (2)$$

in which σ'_{3f} = the failure value of σ'_3 , provided that σ'_1 and σ'_2 are unchanged, i.e., the stress state ($\sigma'_1, \sigma'_2, \sigma'_{3f}$) is to satisfy the failure criterion. When tensile stresses occur, the nonlinearity index as defined by Eq. 2 is less than unity even at failure.

In Eqs. 1 and 2, a failure criterion is involved and in the AXIPLANE program two options exist: (1) The simple and well-known modified Coulomb criterion proposed by Cowan (2); this criterion combines the Coulomb criterion—here with a friction angle equal to 37° —and a maximum tensile stress criterion; and (2) the more accurate, but also more complicated criterion proposed by the writer (10). This latter criterion contains all three stress components and

corresponds to a smooth, convex surface. A comparison of these two criteria with experimental data has been performed by the writer in Ref. 12.

Letting the secant values of Young's modulus and Poisson's ratio depend on the nonlinearity index, the constitutive model predicts the strain hardening before failure, and the failure itself and the strain softening in the post-failure region. Smooth stress-strain curves are obtained, different post-failure behaviors can easily be dealt with, and dilatation is simulated. Any failure criterion can be utilized, and the choice of an accurate criterion by itself assures accurate stress-strain curves. All stress states, including those where there are tensile stresses can be dealt with, as shown in Ref. 11, but path independency is inherent in the model. As described in Ref. 13, the applied implementation of the model in the finite element program results in a behavior corresponding to that of a fracturing solid. This greatly improves the unloading behavior as compared to that of strict nonlinear elasticity.

The model is calibrated to a given concrete by six parameters only, which are all derived from uniaxial tests. These parameters are: the initial elastic parameters, i.e., the initial Young modulus, E_i , and the initial Poisson ratio, ν_i ; the strength parameters, i.e., the uniaxial compressive strength, σ_c ($\sigma_c > 0$); and the uniaxial tensile strength, σ_t ($\sigma_t > 0$); the ductility parameter, i.e., the strain, ϵ_c ($\epsilon_c > 0$), at uniaxial compressive failure; and finally the post-failure parameter, D , that determines the degree of strain softening when the crushing of the concrete occurs.

Through the maximum tensile stress criterion, the modified Coulomb criterion contains in itself a cracking criterion given by $\sigma_1 \geq \sigma_t$. The failure criterion of the writer (10) corresponds to a smooth surface in terms of one equation, and cracking is assumed to occur if: (1) The failure condition is violated; and (2) if $\sigma_1 \geq \sigma_t/2$ holds. This cracking criterion was proposed in Ref. 11, and its close agreement with experimental data is demonstrated in Ref. 12. The crack plane is assumed to be normal to the direction of the principal stress, σ_1 , at the moment of cracking. Once a crack is developed, it is assumed to remain open with a fixed direction. The standard smeared cracking approach is utilized. The shear stiffness along the crack plane is reduced to ηG , in which G = the shear modulus of the concrete; and η = the shear retention factor, $0 \leq \eta \leq 1$. This factor is subject to much dispute, because in reality it is a complicated function of crack-width, relative displacement tangential to the crack plane and the nature of the crack surface. For simplicity, however, we consider the shear retention factor to be a fixed value, and $\eta = 0.01$ is utilized. The predictions obtained in Ref. 13 suggest this value to be sufficiently accurate. A detailed examination of these matters is also given there.

Lok-Test

The configuration of the specific pull-out test considered here, the Lok-Test proposed by Kierkegaard-Hansen (5), is shown in Fig. 1. During application, a test bolt, consisting of a stem and a circular steel disc, is mounted inside the form; see Fig. 1(a). After curing the concrete, the form is stripped, and the stem is unscrewed. At the time of testing, a rod having a slightly smaller diameter than the stem is screwed into the disc and a cylindrical counter pressure is mounted. see Fig. 1(b). The rod is loaded by a mill-out force until failure

where a small piece of concrete can be punched out if sufficient displacement of the rod is applied. As shown in Figs. 1(b) and 2, this piece of concrete has the form of a frustrum of a cone. The meridians are almost straight lines that connect the outer periphery of the disc with the inner periphery of the cylindrical counter pressure.

Experimental data for the Lok-Test have shown a linear relation between the force required to extract the embedded steel disc, and the uniaxial compressive strength of the concrete. A general status of the various experimental investigations has been given recently by Kierkegaard-Hansen and Bickley (6).

RESULTS

Fig. 3 shows the analyzed structure, as well as the axisymmetric finite element mesh consisting of 441 triangular elements. The elements that represent the steel disc appear in this figure. Perfect bond between the steel and the concrete is assumed. The pull-out force, as well as the boundary conditions at the location of the cylindrical counter pressure, are also indicated.

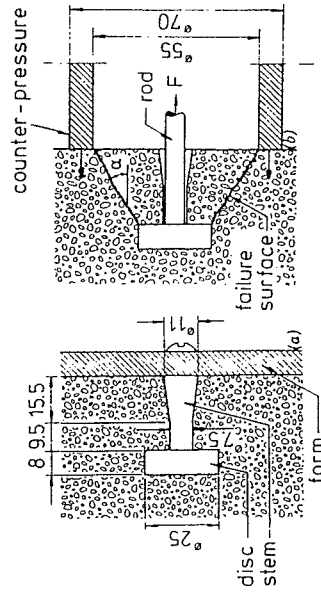


FIG. 1.—Application and Configuration of Lok-Test (All Dimensions Are in millimeters)

To begin with, some important aspects of the structural behavior of the Lok-Test will be illustrated. Special attention will be given to the failure mode. After that, the influence of some concrete material data will be investigated in detail. In the first place, the failure criterion of the writer (10) is utilized; later the effect of using the modified Coulomb criterion is evaluated.

To illustrate the structural behavior, we use concrete material data that can be considered as quite representative and realistic. For this purpose we approximate the behavior of a specific concrete tested by Kupfer (7). The constitutive model of this relatively strong concrete is calibrated by the following parameters, all in accordance with experimental data: $E_c = 3.24 \times 10^4$ MPa; $\nu_c = 0.2$; $\sigma_c = 31.8$ MPa; $\sigma_c/\sigma_e = 0.10$; $\epsilon_c = 2.17\%$; and $D = 0.2$. Using these data, the normalized stress-strain curve is shown in Fig. 4. The values $E = 2.05 \times 10^7$ MPa, and $\nu = 0.3$ were employed for the steel disc.

Let us first consider the predicted development of radial and circumferential cracks as the loading increases. This is shown in Fig. 5, where the loadings are expressed in relation to the predicted failure load. The analysis determines cracking in terms of cracked elements alone. Therefore, some arbitrariness is

necessarily involved when visualizing circumferential cracking as discrete cracks. However, cracking initiates as circumferential cracks behind the disc at 7% loading. This type of cracking appears in Fig. 5(a), and is caused directly by the pull-out force. At 18% loading, radial cracking initiates at the annulus near the outer concrete surface. These cracks are caused by flexure similar to the bending of plates. Such radial cracks appear in Fig. 5(b). With increased loading, the cracks shown there develop gradually. However, at 64% loading a considerable development of new circumferential cracks occur. As shown in Fig. 5(c), these new circumferential cracks extend from the outer part of the steel disc towards the support. It is of interest to note that even though the concrete is severely cracked, its carrying capacity is far from being exhausted. Therefore, it is obvious that only very little of the pull-out force is carried directly by tension in the concrete. Increased loading, in particular, causes the radial cracks to develop; the crack pattern just before predicted failure is shown in Fig. 5(d).

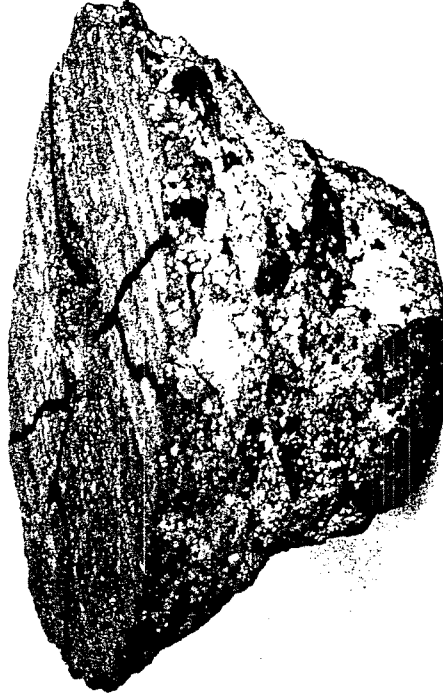


FIG. 2.—Punched-Out Piece of Concrete (Cracks Are Made Visible Using Pencil Tracing)

While the predicted circumferential cracks are supported by experimental evidence [compare Figs. 1(b) and 2], radial cracks have not been observed experimentally prior to the present study. However, whereas the region theoretically exposed to radial cracking is quite large, the corresponding crack widths are estimated to be quite small. If it is conservatively assumed that all tangential deformation is concentrated in only one radial crack, then just before failure this crack width is around 0.05 mm that is hardly visible. Moreover, the stresses are unloaded and crack widths reduced after failure, thereby supporting the conclusion that no radial cracks are directly visible on the punched-out piece of concrete. However, close inspection of such concrete specimens using a microscope reveals that clear radial cracking is indeed present. Such cracking is visualized on the specimen in Fig. 2 using pencil tracing.

To further illustrate the structural behavior of the Lok-Test, the stress

distribution of the three principal stresses is considered at 70% loading, i.e., the cracking is slightly more developed than indicated in Fig. 5(c). This stress distribution is shown in Fig. 6, in which isostress curves are shown and the directions of the principal stresses in the RZ plane are given at each nodal point. In accordance with the radial crack development, the distribution of the tangential stresses shows large regions where tension exists. Only at the support, and notably around the disc do compressive tangential stresses exist. The distribution of the maximum principal stress in the RZ plane also indicates large regions loaded in tension. Only in the vicinity of the disc, and notably at the support do small regions loaded in compression exist. The distribution of the minimum principal stress in the RZ plane is very interesting. Recalling

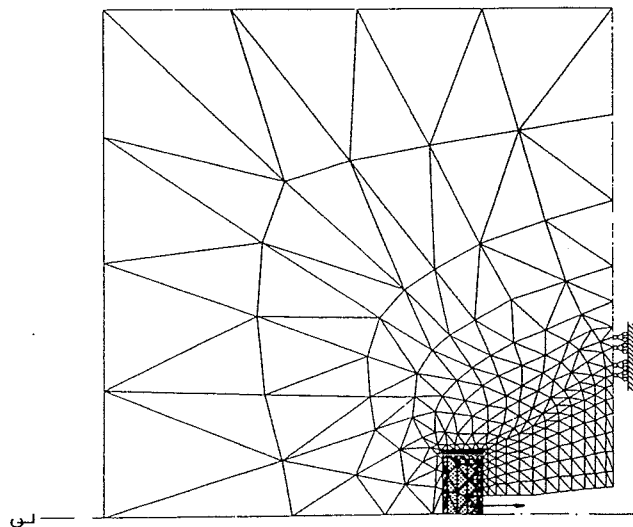


FIG. 3.—Axisymmetric Finite Element Mesh of Lok-Test

that the uniaxial compressive strength of the concrete is 31.8 MPa, and noting that the loading is 70% of the predicted failure load, it appears that large stresses are present at the annulus near the disc. In fact, triaxial compression exists here. Moreover, large compressive stresses are found at the outer periphery of the steel disc, and comparison with the preceding figures shows that biaxial compression occasionally superposed by a small tensile stress appears in this region. Noting the stress directions, it is apparent that large compressive forces run from the disc in a rather narrow band towards the support, where triaxial as well as biaxial compression exist. This carrying mechanism is supported by the crack pattern of Figs. 5(c) and 5(d). It is of interest to note that both the circumferential cracks and the stress directions describe curves that have

a slight curvature even though they are almost straight. This small curvature is also observed in practice; compare to Fig. 2.

In conclusion, Fig. 6 shows that the stress distribution is very inhomogeneous. At increasing loading, a considerable redistribution of stresses can therefore be expected. This suggests strain softening of the concrete in the post-failure region to be of importance for the failure load. Moreover, Fig. 6 shows that large compressive forces run from the disc in a rather narrow band towards the support, and this constitutes the load-carrying mechanism. The stress states in this band are primarily biaxial compression occasionally superposed by small tensile stresses.

As demonstrated previously in Ref. 13, the severity of the stress states is conveniently illustrated by means of the nonlinearity index, β , relating the actual stress state to the failure surface; compare Eqs. 1 and 2. For compressive loading, $0 \leq \beta < 1$, $\beta = 1$, and $\beta > 1$ correspond to stress states located inside, on, and outside the failure surface, respectively. Fig. 7 shows the

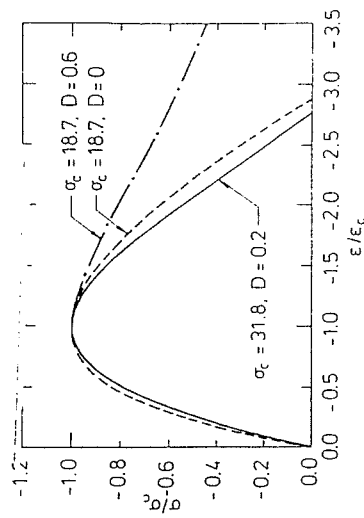


FIG. 4.—Normalized Stress-Strain Curves for Concretes Considered (Strengths Are Measured in megapascals)

development of the contour lines with increasing loading for the nonlinearity index, as a percentage. The distribution in Fig. 7(b) corresponds to the stress distribution given in Fig. 6. Fig. 7 supports the preceding observations that the region at the annulus adjacent to the disc is severely loaded, and this holds also for the region along the outer periphery of the disc. Moreover, the severely loaded narrow band running from the outer periphery of the disc towards the support is very apparent. It should be recalled that when tensile stresses are present, the nonlinearity index is less than unity even at failure; compare to Eq. 2. At 64% loading, strain softening initiates below the steel disc, both adjacent to the annulus and at the outer periphery of the disc. At 79% loading, strain softening develops from the outer periphery of the disc towards the support. This development is pronounced at 88% and also at 100% loading; the latter is the failure load, and the distribution given by Fig. 7(d) corresponds to the last iteration before the calculations were terminated. At the failure load, considerable strain softening occurs also at the disc adjacent to the annulus. This can be observed as a decrease in the nonlinearity index; compare Figs.

7(c) and 7(d). More important, however, is the strain softening occurring in the narrow region adjacent to the outer periphery of the disc, and running towards the support. This strain softening appears as a considerable drop of the nonlinearity index. This effect is very pronounced when comparing Fig. 7(c) with Fig. 7(d), but a comparison of Fig. 7(b) with Fig. 7(c) already shows this tendency. It is important to realize that this gradual decrease of the nonlinearity index due to strain softening in the post-failure region corresponds to the crushing of the concrete. Thus, even though small tensile stresses may exist in addition

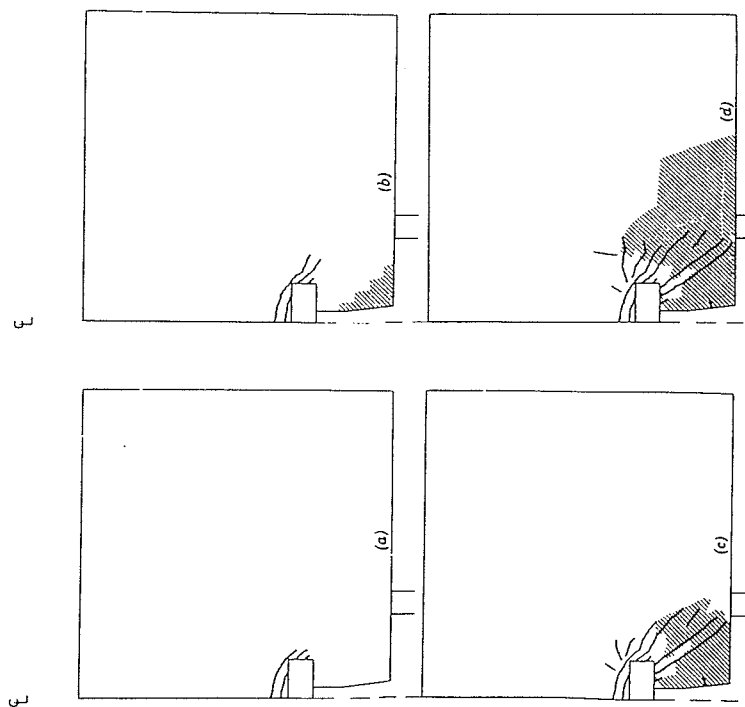


FIG. 5.—Crack Development with Increasing Loadings (Loading Is Expressed in Relation to Predicted Failure Load): (a) Loading = 15%; (b) Loading = 25%; (c) Loading = 64%; (d) Loading = 98%

to the primary biaxial compressive stress states, the failure is caused by the crushing of the concrete and not by cracking. This mechanism is in accordance with the experimentally observed ductile failure mode. Therefore, the force required to extract the embedded disc in a Lok-Test is directly dependent on the compressive strength of the concrete in question. However, the tensile strength may have some direct influence, as will be examined later on.

Let us now compare the predicted failure load with experimental data. Based on the results of different test series, including a total of 1,100 Lok-Tests, Kierkegaard, Hansen and Dickson (6) presented the following results:

pull-out force, F , and uniaxial compressive cylinder strength, σ_c ; $F = 5 + 0.8 \sigma_c$, in which F and σ_c are measured in kilonewtons and megapascals, respectively. This relation is shown in Fig. 8, and is based on concrete mixes, in which σ_c ranges from 6 MPa–53 MPa. The failure load resulting from the present calculation, in which $\sigma_c = 31.8$ MPa, is also indicated. The analysis underestimates the experimental failure load by only 1%.

To investigate the dependence of the σ_c value, a calculation was performed with data from another, weaker concrete. To ensure use of realistic concrete

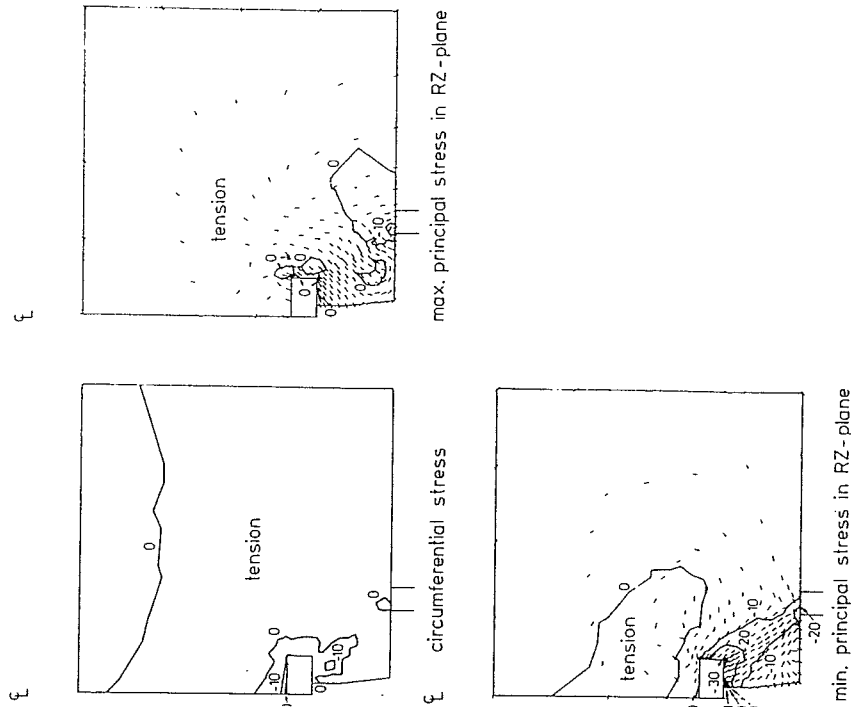


FIG. 6.—Isostress Curves and Directions of Three Principal Stresses at 70% Loading (Quantities Are in megapascals)

data, test results of Kupfer (7) were utilized again. In the constitutive model, the following parameters were applied: $E_c = 2.89 \times 10^4$ MPa; $\nu_c = 0.19$; $\sigma_c = 18.7$ MPa; $\sigma_c / \sigma_{ic} = 0.10$; $\epsilon_c = 1.87\%$; and $D = 0.6$. The close agreement of the resulting predictions with the experimental data of Kupfer (7) has previously been demonstrated in Ref. 11. In general, the weaker the concrete, the more ductile is its post-failure behavior; compare to, e.g., Hognestad, et al. (3). This

stress-strain curve from the aforementioned data is shown. The predicted failure load using these concrete parameters underestimates the actual failure load by only 3%, and is plotted in Fig. 8. Therefore, the calculations are in agreement with the experimental evidence, showing that within the considered variation of the σ_c values, a linear relation exists between pull-out force and compressive strength.

It is remarkable that the prolongation of the experimental line in Fig. 8 intersects the ordinate axis at some distance from the origin. However, two aspects of

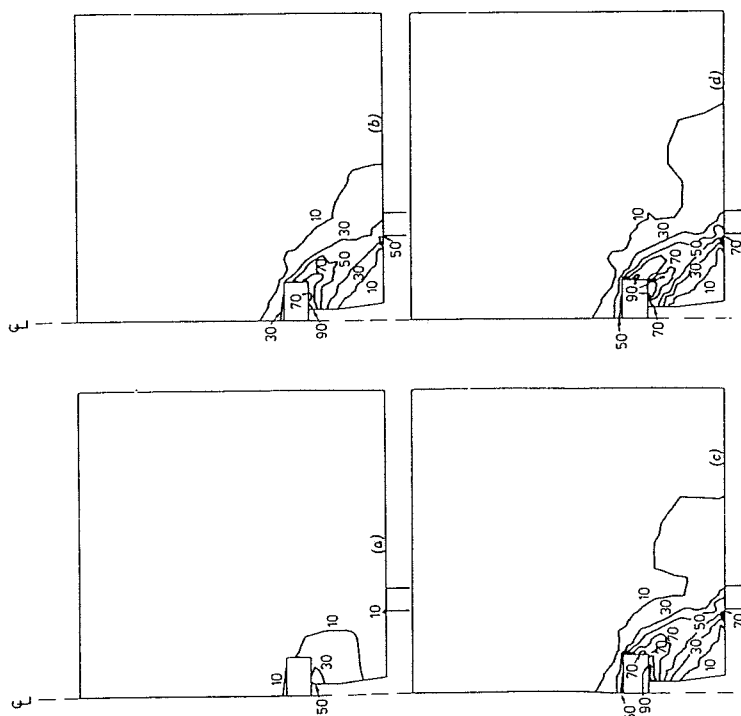


FIG. 7.—Development of Contour Lines for Nonlinearity Index, as a Percentage (Loadings Expressed as a Percentage of Predicted Failure Load): (a) Loading = 20%; (b) Loading = 70%; (c) Loading = 94%; (d) Loading = 100%

concrete behavior are dependent on compressive strength, namely the ductility and the ratio of tensile to compressive strength. As has already been touched upon, the weaker the concrete, the more ductile the post-failure behavior. To investigate the influence of minor variations in the post-failure behavior of the concrete, a calculation was performed using again the concrete having a strength of 18.7 MPa, and possessing unchanged properties except for a lesser ductility. Therefore, the value $D = 0$ was used instead of the more realistic one, $D = 0.6$; compare to Fig. 4. This in fact decreases the predicted failure load by 5%, as shown in Fig. 8. That the failure load depends on the particular

softening behavior of the concrete is indeed to be expected, considering the very inhomogeneous stress distribution.

In general, the weaker the concrete, the larger is the ratio of tensile to compressive strength; compare to, e.g., Wastiels (16). Let us investigate this effect using the concrete having $\sigma_c = 18.7$ MPa, and $D = 0.6$ again, but putting now $\sigma_t/\sigma_c = 0.12$, instead of $\sigma_t/\sigma_c = 0.10$. This increases the predicted failure load by 11%, as shown in Fig. 8. In reality, Kupfer (7) determined the σ_t/σ_c ratio to be 0.105 for the concrete considered, and if interpolation is performed between the two calculations having the σ_t/σ_c ratio equal to 0.10 and 0.12, respectively, then the resulting failure load is 0.7% below the actual value. Even though the tensile strength of the concrete certainly has an influence on the failure load of a Lok-Test, it is of importance to realize that this influence is an indirect one. Only very little of the pull-out force is carried directly by

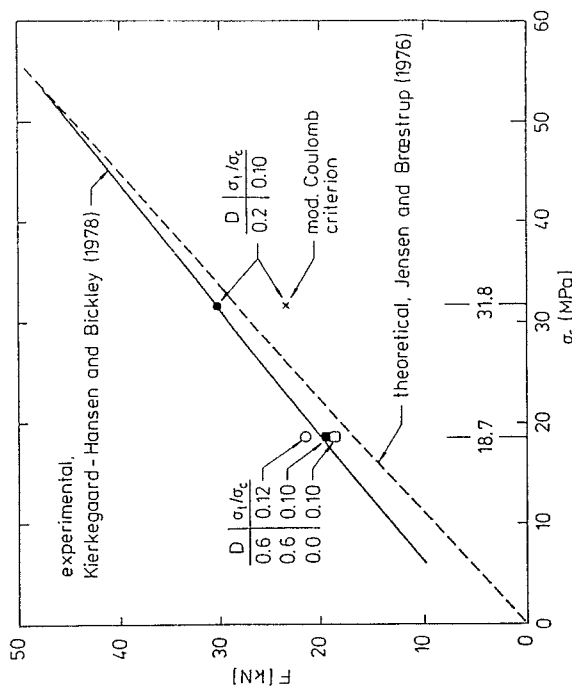


FIG. 8.—Experimental Data Compared with Theoretical Failure Values

tension in the concrete, but the regions where failure takes place are primarily in biaxial compression, occasionally superposed by small tensile stress. The failure is caused by crushing, but the existence of even a small tensile stress considerably decreases the failure strength.

The preceding analysis has demonstrated that the reason that the relation between pull-out force and compressive strength is linear and not proportional is a result of the increasing ductility and the increasing ratio of tensile to compressive strength, the weaker the concrete.

Let us now investigate the influence of different failure criteria. For this purpose we return to the concrete having $\sigma_c = 31.8$ MPa. All constitutive parameters are unchanged, but now the modified Coulomb criterion is applied. Compared to the previous analysis, this reduces the predicted failure load by

23%, as shown in Fig. 8. However, at failure, the critical regions are loaded primarily in biaxial compression, and the modified Coulomb criterion is known to underestimate the failure stresses for such stress states by 25%–30%.

It is of interest to observe that the decrease of failure load, when using the modified Coulomb criterion, is in accordance with the finding that the Lok-Test depends directly on the compressive strength of the concrete and not on its tensile strength. As demonstrated in Ref. 12, the modified Coulomb criterion, in general, underestimates the failure stresses, when concrete is loaded in compression, except when extremely large triaxial compressive stress states exist. Moreover, as shown there, this criterion, in general, overestimates the failure stresses when tensile stresses are present. Therefore, if the failure in a Lok-Test was caused by tensile cracking, then use of the modified Coulomb criterion would result in an increased failure load. However, in accordance with the preceding analysis, use of the modified Coulomb criterion decreases the failure load.

Jensen and Braestrup (4) have previously determined the failure load for a Lok-Test using rigid-ideal plasticity theory. They also used the modified Coulomb criterion, and their result is shown in Fig. 8. It appears that close agreement is obtained even though proportionality and not just linearity between the pull-out force and the compressive strength was obtained. However, the failure load determined by Jensen and Braestrup (4), when $\sigma_c = 31.8$ MPa, is considerably larger than the one determined here when using the modified Coulomb criterion also. This is particularly conspicuous, because Jensen and Braestrup (4), in their analysis, are forced to use a friction angle equal to the angle α shown in Fig. 1(b). This results in a friction angle, $\phi = 31^\circ$. The present finite element analysis is based on the value $\phi = 37^\circ$ which, as previously examined, results in some underestimate of the actual failure stresses. Use of the value $\phi = 31^\circ$ would indeed infer a considerable underestimate of actual failure stresses. However, Jensen and Braestrup (4) in reality compensate for this, as their analysis is based on rigid-ideal plasticity with no softening effects at all. Consequently, they assume failure all along the plane running from the outer periphery of the disc towards the inner periphery of the support. Previous examinations related to Fig. 7 have refuted such an assumption. However, in accordance with findings in Ref. 13, this underlines the extreme importance of including a suitable strain softening behavior in constitutive modeling of concrete.

CONCLUSIONS

In the present paper, which takes advantage of Ref. 12, the structural behavior of a specific pull-out test, i.e., the Lok-Test, has been investigated in detail. Severe cracking occurs, and the stress distribution is very inhomogeneous. It has been shown that large compressive forces run from the disc in a rather narrow band towards the support, and this constitutes the load-carrying mechanism. Moreover, the failure in a Lok-Test is caused by the crushing of the concrete and not by cracking. Therefore, the force required to extract the embedded steel disc is directly dependent on the compressive strength of the concrete in question. However, as the stress states, in which failure takes place, are primarily biaxial compressive occasionally superposed by small tensile stresses

the tensile strength of the concrete has some indirect influence. The effect of strain softening in the post-failure region is important. In general, weak concrete compared to strong concrete has a relatively larger tensile strength and a higher ductility. This explains why the relation between the failure pull-out force and the compressive strength is linear and not proportional.

With respect to finite element modeling, it has been demonstrated that not only is use of an accurate failure criterion important, but modeling of the strain softening in the post-failure region turns out to be a mandatory prerequisite for realistic structural predictions.

APPENDIX.—REFERENCES

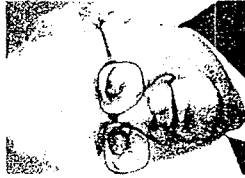
1. Clifton, J. R., "Nondestructive Tests to Determine Concrete Strength—A Status Report," *NBSJR 75729 (PB 246858)*, Materials and Composites Section, National Bureau of Standards, Washington, D.C., July, 1975.
2. Cowan, H. J., "Strength of Plain, Reinforced and Prestressed Concrete under Action of Combined Stresses, with Particular References to the Combined Bending and Torsion of Rectangular Sections," *Magazine of Concrete Research*, London, England, Vol. 5, No. 14, Dec., 1953, pp. 75–86.
3. Hognestad, E., Hanson, N. W., and McHenry, D., "Concrete Stress Distribution in Ultimate Strength Design," *Proceedings*, American Concrete Institute, Vol. 52, No. 4, Dec., 1955, pp. 455–479.
4. Jensen, B. C., and Braestrup, H. W., "Lok-Tests Determine the Compressive Strength of Concrete," *Nordisk Betong*, Stockholm, Sweden, No. 2, 1976, pp. 9–11.
5. Kierkegaard-Hansen, P., "Lok-Strength," *Nordisk Betong*, Stockholm, Sweden, No. 3, 1975, pp. 19–28.
6. Kierkegaard-Hansen, P., and Bickley, J. A., "In-Situ Strength Evaluation of Concrete by the Lok-Test System," presented at the Oct. 29–Nov. 3, 1978. American Concrete Institute Fall Convention, held at Houston, Tex.
7. Kupfer, H., "Das Verhalten des Betons unter Mehrachsigen Kurzzeitbelastung unter besonderen Berücksichtigung der Zwiachsigen Beanspruchung," *Deutscher Ausschuss für Stahlbeton*, Berlin, West Germany, Vol. 229, 1973.
8. Mailhot, G., Bisailon, A., Carrette, G. G., and Malhotra, V. M., "In-Place Concrete Strength: New Pullout Methods," *Proceedings*, American Concrete Institute, Vol. 76, No. 12, Dec., 1979, pp. 1267–1282.
9. Malhotra, V. M., "Evaluation of the Pull-Out Test to Determine Strength of In-Situ Concrete," *Materials and Structures*, Vol. 8, No. 43, Jan.–Feb., 1975, pp. 19–31.
10. Ottosen, N. S., "A Failure Criterion for Concrete," *Journal of the Engineering Mechanics Division*, ASCE, Vol. 103, No. EM4, Proc. Paper 13111, Aug., 1977, pp. 527–535.
11. Ottosen, N. S., "Constitutive Model for Short-Time Loading of Concrete," *Journal of the Engineering Mechanics Division*, ASCE, Vol. 105, No. EMI, Proc. Paper 14375, Feb., 1979, pp. 127–141.
12. Ottosen, N. S., "Nonlinear Finite Element Analysis of Concrete Structures," thesis presented to the Technical University of Denmark, at Copenhagen, Denmark, in 1980, in partial fulfillment of the requirements for the degree of Doctor of Philosophy *Risø-R-411*, Risø National Laboratory, Roskilde, Denmark.
13. Ottosen, N. S., "Finite Element Analysis of Plane and Axisymmetric RC Structures," submitted for publication, Feb., 1980.
14. Skramstjær, B. G., "Determining Concrete Strength for Control of Concrete in Structures," *Proceedings*, American Concrete Institute, Vol. 34, Jan.–Feb., 1938, pp. 285–303.
15. Temper, B., "The Measurement of Concrete Strength by Embedded Pull-Out Bars," *Proceedings*, American Society for Testing and Materials, June, 1944, pp. 880–887.
16. Wastels, J., "Behaviour of Concrete under Multiaxial Stresses—A Review," *Cement and Concrete Research*, Vol. 9, Jan., 1979, pp. 35–44.

PULLOUT TESTING OF CONCRETE

Historical Background and Scientific Level Today

Herbert Krenchel, Dr. techn.,
Department of Structural Engineering, ABK,
Technical University of Denmark, DTH, Denmark

John A. Bickley, ACI-fellow,
Concrete technology consultant for the Trow
Group Ltd., Brampton, Ontario, Canada.
Member of ACI committees: 214, 228 and 362.



ABSTRACT

A survey of the different pullout systems developed for controlling concrete strength with an examination of stress- and strain-distribution inside the concrete at peak load by the Scandinavian pullout testing system.

Key words: pullout testing, compressive strength, fracture mechanic, internal micro-cracking, acoustic emission activity.

1. INTRODUCTION

Concrete pullout tests are considered non-destructive. The part of the concrete structure damaged by the test is normally so small that it can be easily repaired. Furthermore, in many cases, it is not necessary to continue the test to final rupture. Testing can be terminated when the required strength level has been reached in the concrete in which case the test is fully non-destructive. Even in cases where inserts are loaded to failure they can generally be left in place and no sensible damage occurs to the structure.

Different pullout, pulloff or break-off systems have been developed over the years for determining concrete strength. In most cases these methods have not been scientifically developed and did not therefore produce a reliable correlation to the material property of primary interest to the building industry: the concrete compressive strength.

2. DEVELOPMENT

2.1 Russian Pullout Tests

During the years 1934-1938 intensive research was going on in the Soviet Union with the aim of determining the strength of concrete in completed structures. Several different systems were suggested, the simplest and most promising method, it now appears, being the pullout test system suggested by I. V. Volf, Charckov, and (almost simultaneously) by O. A. Gershberg, Moscow, as described in

NORDIC CONCRETE RESEARCH



1938 by B. G. Skramtajev, /1/.

This method consists of embedding a specially shaped steel rod with a spherically thickened end into the concrete during casting, see Fig. 1. The steel rod has a diameter of 8 mm and the spherical end - 12 mm, the centre of the sphere being placed 44 mm below the concrete surface so that full length of the rod in the concrete is about 50 mm.

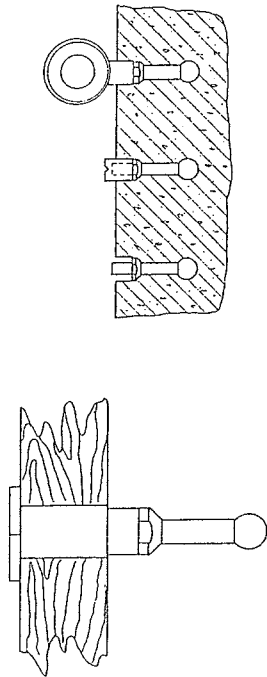


Fig. 1 Specially shaped steel rods with spherically thickened ends for the Russian pullout testing system (Volf and Gershsberg, 1934/38).

Testing for concrete strength is carried out by pulling out the rod in its longitudinal direction vertically to the concrete surface by means of a special dynamometer placed on the concrete surface. In this way a cone of concrete is pulled out with the rod, the top of the cone laying nearly in the centre of the sphere and with generating lines starting at an angle of approximately 45 degrees to the axis of the bolt, but running out near the concrete surface to a maximum diameter of about 10-12 cm, see Fig. 2 and 3.

Volf carried out series of experiments to determine the relation between the concrete cube strength R_c and the maximum load at rupture P (the pulling effort). In 1938 such calibrations had only been carried out with very low strength concrete (R_c from 1.5 to 10.8 MPa). These tests showed a simple linear correlation between P (in kg) and R_c (in kg per sq.cm): $K = \frac{P}{R_c} = 9.5$.

Experiments with higher strength concrete would have shown whether the coefficient K remains a constant or varies with the strength of the concrete. Such test results have, as far as is known, not been published. From the principle of this test system and from the shape of the rupture cone as shown in Fig. 3, it seems clear that the pullout force P in these tests must have been more directly related to the concrete *tensile* strength than to the compressive strength. With this test system the coefficient K will decrease drastically with increasing concrete compressive strength. It is not likely that it would be possible with normal types of concrete (compressive strength σ_c between

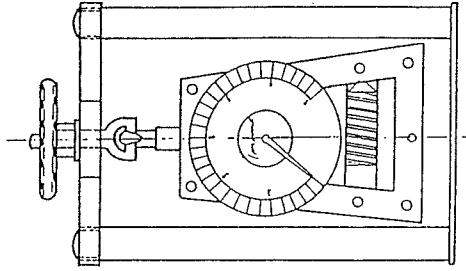


Fig. 2 Special dynamometer for pullout tests according to Fig. 1.

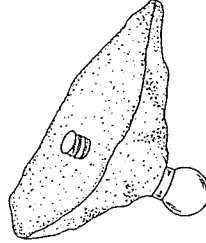


Fig. 3 Steel rod and concrete cone from pullout test according to Fig. 1 and 2.

20 and 50 MPa f.inst.) to predict indirectly with any reasonable confidence the compressive strength of the material from this type of pullout tests.

2.2 Pulloff Test By Glueing

Some thirty years ago different types of two-component epoxy glue came on the market. These are very efficient cold setting organic cements ideal for fixing metal components directly to a concrete surface f.inst. The adhesion properties of this glue or cement far exceed the tensile strength of even the strongest type of Portland cement concrete. At several laboratories, all over the world, different test systems were suggested and tried out on this basis.

A disc or stiff plate was glued onto the concrete surface and pulled or broken off later, when the glue had set. Such tests have been mentioned sporadically in the literature from time to time since then. It seems that there is only limited interest in this testing principle today because of the high scatter in the test results obtained and the poor correlation which is always found in such tests between the pull-off load and the concrete compressive strength, see Fig. 4. (The results are no doubt more directly correlated to the concrete *tensile* strength).

3. POST WORLD WAR II DEVELOPMENT

In the 60's and 70's renewed interest in pullout testing was created by the works of Kaindl, Kierkegaard-Hansen, Malhotra, Richards, and Tremper.

3.1 Pullout Testing With Steel Disc

During the years 1960-70 P. Kierkegaard-Hansen (Denmark) developed the so-called LOK-TEST method, a pullout testing system giving a reliable in-situ determination of the concrete compressive strength.

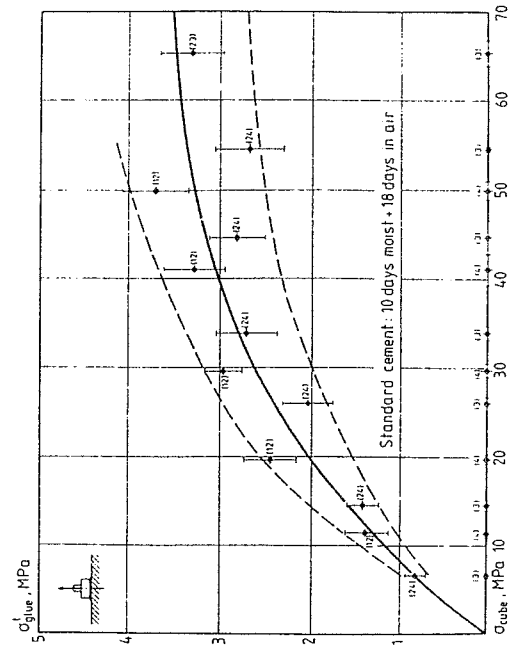


Fig. 4 Results from pulloff tests by glueing. (Efsen and Krenchel, 1953/54).

This test system has some resemblance with the old Russian method by Volf and Gershberg, but it is of a better design giving no premature failure inside the concrete at the head of the pullout bolt and, further, what is a significant improvement, the top angle of the rupture cone has been chosen so that a direct linear relationship is obtained with close correlation between the pullout force and the concrete compressive strength.

With this system a thick 25 mm circular steel disc (1) is fixed by a special bolt (2) and screw (3) on the inside of the form before casting the concrete. The bolt or stem holds the disc at a distance of 25 mm from the inside of the form with its axis perpendicular to the concrete surface, see Fig. 5.

Just before stripping the form the screw (3) is loosened so that disc and bolt stays inside the concrete.

On the day of testing the bolt (2) is replaced by a 7.5 mm bolt of high-tensile steel and a small 7 tons capacity hydraulic jack is placed on the concrete surface and connected to the tensile bolt. The jack rests on the concrete surface and applies force through a counter-pressure ring. The inside diameter of this ring and the outside diameter of the steel disc determine the geometry of the final pullout cone.

When Kierkegaard-Hansen carried out his first tests according to this system some twentyfive years ago, the inside diameter of the counter-pressure ring in his first test set-up was substantially bigger than today (130 mm instead of 55 mm). The calibra-

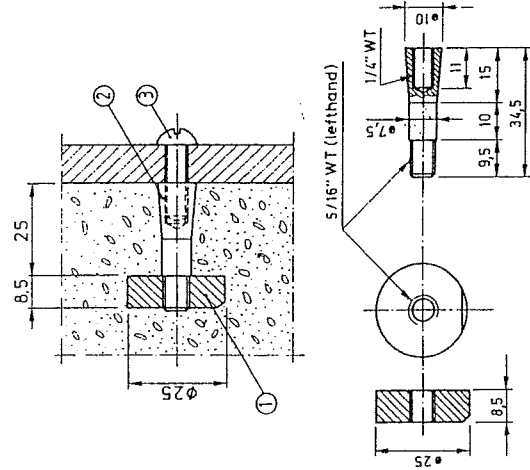


Fig. 5 Pullout disc and bolt fixed on inside of form before casting the concrete.

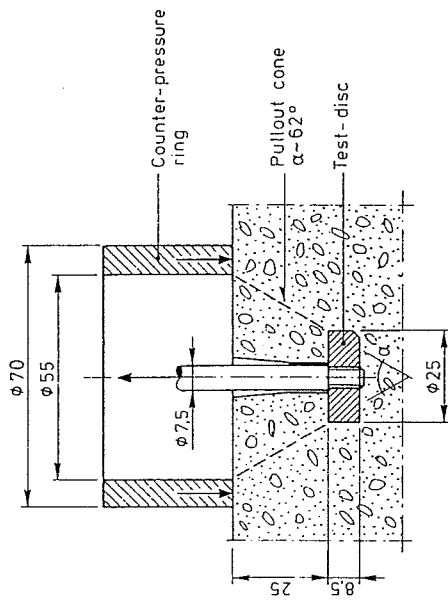


Fig. 6 Test set-up for the so-called LOK-TEST pullout system. (Dimensions in mm).

tion curve he then obtained between pullout force and concrete quality showed more or less direct correlation to the concrete tensile strength as with the pullout testing systems mentioned above. By systematically reducing the inside diameter of the counter-pressure ring step by step keeping all other dimensions fixed he finally found that a direct correlation to the concrete compressive strength is obtained when the top angle of the pullout cone is about 62° , see Fig. 6.

3.2 Further Development

A drawback with the above system, is that it can only be used where the special test discs have been cast into the concrete beforehand. In order to be able to use the system after casting the concrete, C. Germann Petersen (Denmark) seven years ago developed the so-called CAPO-TEST.

The principle here is that a hole 18 mm diameter and about 45 mm deep is first drilled in the concrete perpendicularly to the surface. After this a groove is cut out in the concrete with a special milling equipment. This groove has a diameter of 25 mm and is 10 mm high. It is formed 25 mm below the concrete surface, see Fig. 7.

A special expanding steel disc with an outside diameter of 18 mm is then placed on a bolt and put into the hole down to the level of the groove. By turning the bolt with two wrenches (the bolt consists of an inside and an outside part) the steel disc is expanded, until it reaches the inside diameter of the groove, see Figures 8 and 9. Finally the pullout jack mentioned above is placed in top of the equipment and connected with the pull

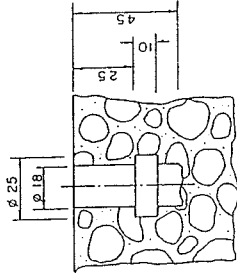


Fig. 7 Hole and groove drilled out for the so-called CAPO-TEST pullout system. (Dimensions in mm).

bolt. A pullout test is then made in the same way with the same system, the same geometry inside the concrete, and with the same top angle in the pullout cone.

3.3 Correlation With Compressive Strength

In construction, the property of concrete which is required to be determined in order to remove forms, post-tension, remove shores, or terminate curing is the compressive strength of the concrete. Since it is universally accepted that the compressive strength of the concrete is determined by testing standard specimens (cylinders or cubes) it is necessary for any non-destructive test system used to be correlated with the standard test specimens so that the answer obtained by the non-destructive test is a measure of the compressive strength of the concrete in place.

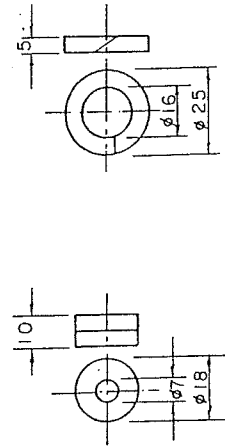


Fig. 8 Special expanding steel disc for the CAPO-TEST system. (Dimensions in mm).

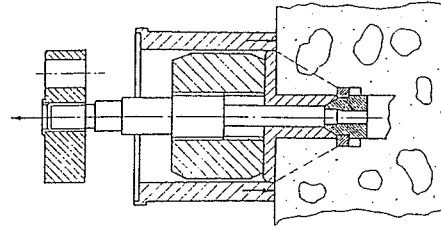


Fig. 9 Test set-up for the CAPO-TEST system.

The pullout system mentioned has been intensively examined since then by several laboratories all over the world, /2/, /3/, /4/, (with most relevant references from the period). It is interesting to see what little influence the different parameters such as type of cement, type of aggregate and curing conditions have on the calibration curve, the spread in the test results, and the coefficient of correlation.

For concrete with a compressive strength (determined on 150 x 300 mm test cylinders) from 15 MPa to 85 MPa (maximum capacity of the instrument) the calibration curve is linear and a coefficient of correlation of between 0.90 and 0.95 is normally obtained. Even major changes in the curing conditions have shown practically no influence on the position of the calibration curve.

The linear calibration curve in combination with the high coefficient of correlation indicates that rupture at pull-out loading in this test system is caused by the compression straining in the truncated area between the top face of the steel disc and the bottom face of the counter-pressure ring.

On the basis of, say, five tests carried out on a given sample of concrete the compressive strength of the material is predicted with a maximum deviation of ± 4 MPa (95% confidence limits). If twenty tests are carried out on the same concrete the deviation will be only ± 2 MPa.

3.4 Correlation Data

In 1979 large scale calibration tests were carried out at the Technical University of Denmark (Department of Structural Engineering) with both types of pullout methods in parallel /5/.

Thirty different test series were carried out with each of the two test methods, the concrete compressive strength (cylinders: 150 mm diameter x 300 mm) varying from 3.3 MPa to 74.0 MPa. The result of these calibration tests appears in Table 1, where σ_c is the average compressive strength of the concrete, v the coefficient of variation and n the number of compressive tests, on which σ_c and v are determined. L is the average pullout load in each series of LOK-tests and C the average pullout load from the CAPO-tests, v and n , again, being coefficient of variation and number of tests in these figures, respectively.

It will be seen that for normal types of concrete (compressive strength above, say, 10 MPa) the coefficient of variation in the compression tests was between 2.3 and 6.6%, in the LOK-tests between 1.6 and 14.9% and in the CAPO-tests between 2.6 and 12.9%.

The calibration curves from these tests are shown in the diagrams Fig. 10 and 11. It will be seen that in both cases the curves are linear from a concrete compressive strength above 15 MPa. It will further be seen that the coefficient of correlation

Table 1 CALIBRATION TESTS BASED ON 128 COMPRESSION TESTS (cylinders 150 mm diameter x 300 mm), 240 LOK-tests and 234 CAPO-tests (Department of Structural Engineering, ABK/DTH, 1979)

Series No.	Compressive tests			LOK-tests			CAPO-tests		
	σ_c MPa	v %	n No.	L kN	V_L %	n_L No.	C kN	V_C %	n_C No.
1	28.2	3.1	4	28.7	5.4	8	29.1	6.4	6
2	28.8	2.4	4	30.6	8.3	8	30.0	7.9	8
3	30.8	3.3	4	30.6	6.9	8	30.9	8.2	8
4	30.5	5.5	4	31.3	8.3	8	31.1	10.7	8
5	29.5	3.5	3	33.1	9.1	6	32.3	8.6	6
6	29.4	6.6	3	33.5	6.7	6	32.7	7.8	6
7	14.3	5.0	6	14.9	7.7	12	13.0	9.4	12
8	42.6	3.4	6	39.1	6.4	6	40.6	6.3	6
9	44.2	2.7	6	39.2	6.7	6	39.7	4.6	6
10	42.6	3.4	6	38.8	3.2	6	39.8	3.4	6
11	44.2	2.7	6	38.5	4.3	6	37.9	3.4	6
12	25.4	5.0	6	22.7	7.3	12	21.1	6.1	12
13	37.4	2.3	2	33.0	6.5	4	32.8	2.6	4
14	39.1	3.6	2	35.3	1.6	4	35.1	5.5	4
15	40.2	1.2	2	32.8	5.7	4	30.9	9.3	4
16	40.2	4.0	2	32.0	9.2	4	31.9	6.1	4
17	38.1	4.6	3	35.1	13.0	6	35.8	9.5	6
18	38.6	3.8	3	34.2	7.1	6	35.8	5.4	6
19	32.9	3.8	5	26.9	8.5	12	26.9	8.5	12
20	33.0	3.1	6	30.0	5.6	12	29.1	10.1	12
21	28.8	4.5	4	22.4	14.9	8	25.8	10.8	8
22	26.3	4.1	4	22.7	12.0	8	24.2	7.1	8
23	24.9	3.6	4	22.6	9.8	8	22.9	4.9	8
24	24.7	3.6	6	21.8	6.0	12	21.2	12.9	12
25	42.8	3.1	2	31.8	8.3	4	34.4	8.7	4
26	39.3	3.1	2	31.3	6.2	4	31.8	4.6	4
27	37.1	4.0	2	33.8	7.4	4	35.4	4.7	4
28	74.0	3.5	9	61.6	6.7	24	60.6	5.7	24
29	7.6	3.0	6	8.66	11.9	12	9.04	13.4	12
30	3.3	2.6	6	4.71	16.6	12	3.44	22.7	8
#	Mean	3.9			8.1			7.9	

Note: # This data not included in the weighted mean values as compressive strength range was below 15.0 MPa (see Fig. 10 and 11).

tion in both cases was quite high ($r_{xy} = 0.95$) and that the regression line is practically the same for the two types of tests. With L and C in kN and σ_c in MPa the following results were obtained:

$$\text{LOK-TEST: } L = 4.7 + 0.768 \sigma_c \quad (s = 3.60)$$

$$\text{CAPO-TEST: } C = 5.3 + 0.751 \sigma_c \quad (s = 3.47)$$

where s is standard deviation of the residual.

4 FRACTURE MECHANICS ANALYSIS

The extraordinary close correlation always obtained between the concrete compressive strength and the ultimate load in the LOK- and CAPO-TEST system has puzzled many researchers and put up the following questions: What is the fracture mechanics in the concrete when this type of testing is carried out? What happens inside the concrete when the pullout peak load is reached?

These problems have been examined in different ways over the years: by Jensen and Braestrup in 1976 (plasticity theory), /6/, by Ottosen in 1981 (nonlinear finite element analysis), /7/ by Stone and Carino in 1983 (large scale tests with embedded strain gauges in the concrete), /8/, and by Krenchel and Shah in 1985 (analysis of progressive micro crack formation with simultaneous examination of acoustic emission activity), /9/.

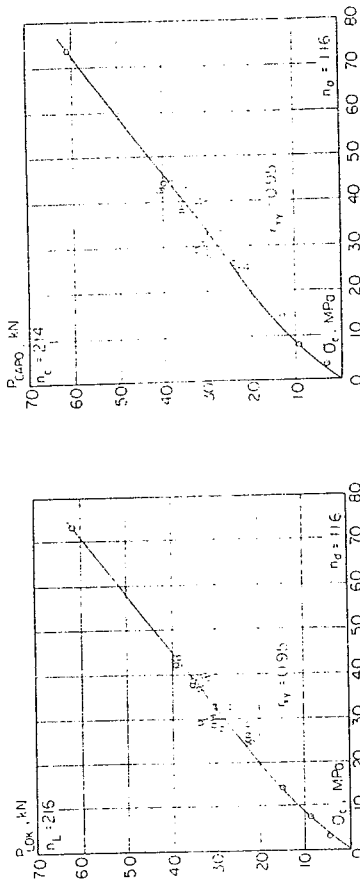


Fig. 10 and 11 Calibration curves from LOK-TEST and CAPO-TEST investigations carried out in 1979 (Technical University of Denmark, Department of Structural Engineering).

4. CONCLUSION

The conclusion today from these theoretical and experimental examinations seems to be, that the internal rupture during this type of test is a multi-stage process, where three different stages with different fracture mechanisms can be clearly separated:

1. In the first stage, at a load level of about 30-40% of the ultimate load, tensile cracks are formed starting from the notch formed by the upper edge of the pullout disc. These cracks are running out in the concrete with a very open angle, (cone angle between 100° and 135°). Total length of this first crack is typically some 15 to 20 mm from the edge of the disc, /10/.

As a result of this first stage cracking the material between the top face of the pullout disc and the bottom face of the counter pressure ring is now free so that straining in the material is now concentrated and all load is taken up in the truncated zone between these two plane faces.

2. In the second stage of internal rupture a multitude of stable microcracks are formed in the above-mentioned truncated zone, the main direction of these cracks running from top of disc to bottom of ring forming a cone angle of approximately 84° , see Fig. 12.

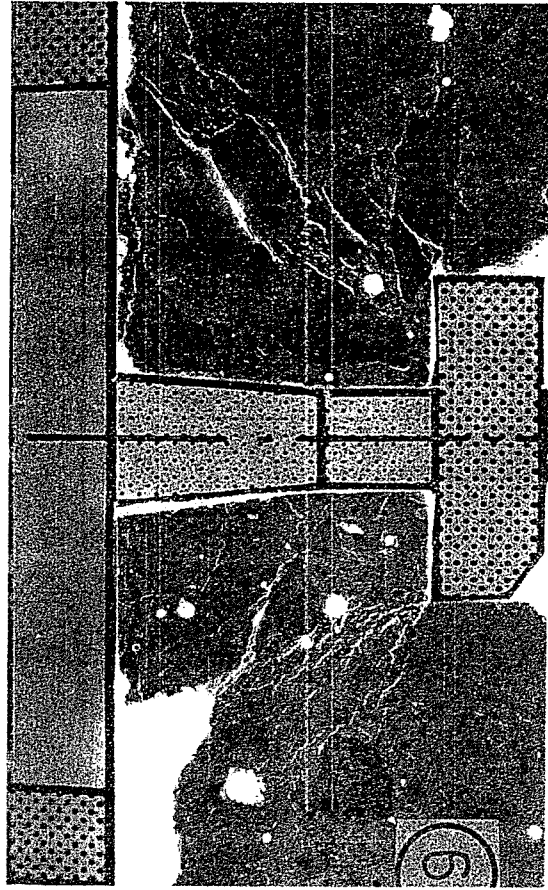


Fig. 12 Crack analysis of pullout test de-loaded from peak of load/displacement curve. Tensile cracking stage No. 1 is seen to the left and multi micro cracking stage 2 to the right. Pullout crack stage 3 has not yet been formed.

The formation of this second cracking pattern is very much parallel to the formation of more and more vertical micro-cracks inside a concrete cylinder or prism during ordinary uniaxial compressive tests, /11/, /12/.

Development of the acoustic emission activity during this second stage of the test also follows an exponential function quite parallel to the AE-development in ordinary uniaxial compressive tests, /9/.

If the pullout jack is specially equipped with transducers for measuring load versus displacement during the test, this second stage of internal microcrack formation could be followed all the way up to and just past the peak of the stress-strain curve.

2. If more and more oil is pumped to the pullout jack, even after the load has stabilized at the peak point, then the third stage of internal rupture occurs by the formation of a tensile/shear crack all the way round, running from the outside edge of the disc to the inside edge of the counter pressure ring and forming the final pullout cone with a cone angle of about 62°, see Fig. 13.

This is followed by a sharp jump in the AE-activity to a level approximately twice as high as it was at the peak of the stress-strain curve. This very high AE-level is kept

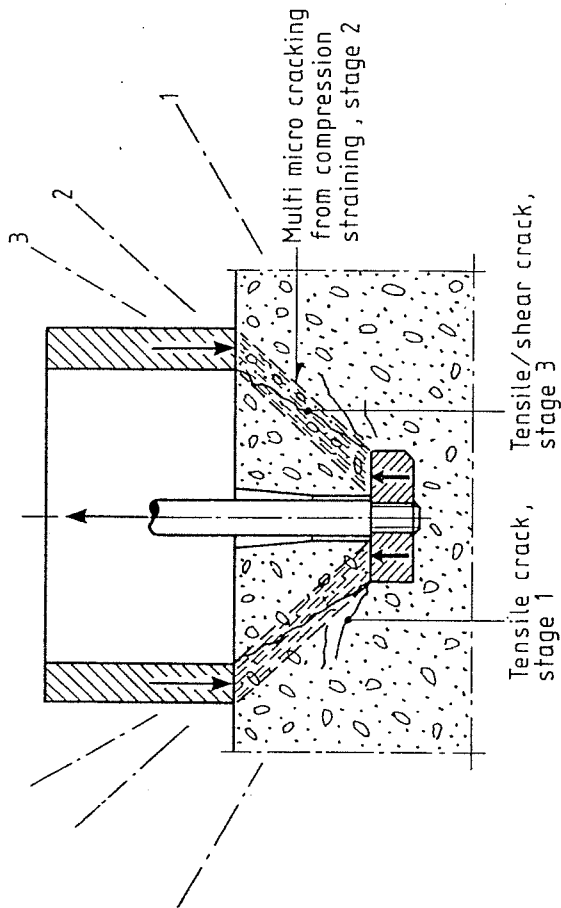


Fig. 13 The three different stages of internal cracking in the concrete during pull-out loading.

constant during the descending part of the stress-strain curve where the concrete cone and the disc is now pulled out.

In most cases of practical testing with this system the oil pressure in the pullout jack is released just after the peak of the stress-strain curve when the load just starts descending, but before the last mentioned type of crack has been developed. In this case the test is fully non-destructive.

As micro cracking stage No. two is responsible for and directly related to the ultimate load in this testing procedure it seems quite logical that such close correlation with the concrete compressive strength is always obtained.

It would be interesting one day to measure the ultimate compressive straining in the center-line of the truncated compression zone (with a cone angle of 84°) and not in the shear zone (cone angle 62°) where maximum compressive straining does not occur in this testing system.

Presumably most confusion regarding the scientific level of this testing system has been introduced by the name: Pullout testing. If this test is carried out correctly with de-loading just after the peak load has been established, no pulling-out occurs. This is a parallel to what happens during ordinary compressive testing of concrete where the cube or cylinder can be taken out in one piece just after the peak load is

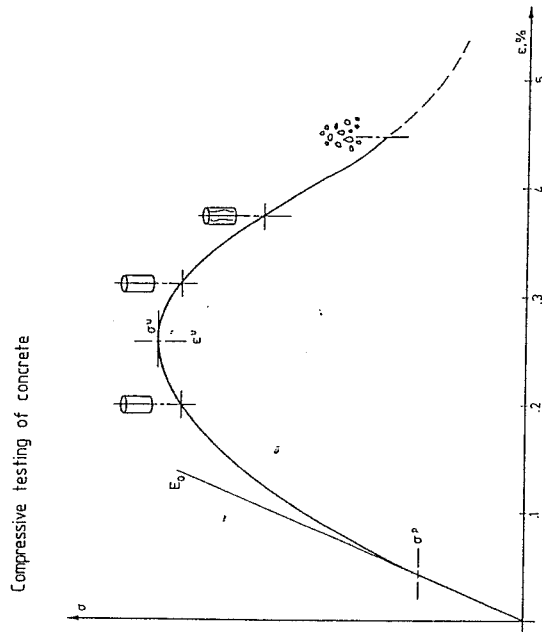


Fig. 14 Stress-strain curve from uniaxial compressive test on plain concrete.

passed. Total crushing of the concrete way down the descending branch of the stress-strain has nothing to do with the internal fracture mechanism at the peak point, where the compressive strength of the material is determined.

REFERENCES

- /1/ Stramtajev, B.G.: Determining Concrete Strength for Control of Concrete in Structures. *ACI-Proceedings*, Vol. 34, (1938), pp. 285-303.
- /2/ Bickley, J.A.: The Variability of Pullout Tests and In-place Concrete Strength. *Concrete International: Design and Construction*, Vol. 4, No. 4, Apr. 1982, pp. 44-51.
- /3/ Petersen, C.G.: LOK-Test and CAPO-Test Development and their Applications. *Proc. Institution of Civil Engineers*, Part 1, May 1984, pp. 539-549.
- /4/ Krenchel, H. and Petersen, C.G.: In-Situ Pullout Testing with LOK-TEST, Ten Years' Experience. Presented at the Research Session of the International Conference on In Situ/Non-Destructive Testing of Concrete, Ottawa, Ontario, October 2-5, 1984, pp. 24.
- /5/ Krenchel, H.: LOK-Testing and CAPO-Testing of Concrete Compressive Strength (in Danish). Department of Structural Engineering (ABK), Technical University of Denmark, Internal Report: I71, 1982.
- /6/ Jensen, B.C. and Brastrup, M.W.: LOK-Test Determines the Compressive Strength of Concrete. *Nordisk Beton*, Journal of the Nordic Concrete Federation (Stockholm), No. 2, 1976, pp. 9-11.
- /7/ Ottosen, N.S.: Nonlinear Finite Element Analyses of Pullout Test. *Proceedings, Journal of the Structural Division, ASCE*, Vol. 107, ST4, Apr. 1981, pp. 591-603.
- /8/ Stone, W.C. and Carino, N.J.: Deformation and Failure in Large-Scale Pullout Tests. *ACI Journal*, Technical Paper, November-December 1983, pp. 501-513.
- /9/ Krenchel, H. and Shah, S.P.: Fracture Analysis of the Pullout Test. *RILEM, Materials and Structures*, Nov.-Dec. 1985, No. 108, pp. 439-445.
- /10/ Ballarini, P., Shah, S.P. and Keer, L.M.: Failure characteristics of short anchor bolts embedded in a brittle material. *Proc. Royal Society of London A404*, 8. March 1986, pp. 35-54.
- /11/ Glucklich, J.: Fracture of plain concrete. *Proceedings of the American Society of Civil Engineers*, Vol. 89, No. EM6, December 1963, pp. 127-139.
- /12/ Shah, S.P. and Slate, F.: Internal Microcracking Mortar-Aggregate bond and the Stress-Strain curve of Concrete. *International Conference: The Structure of Concrete*. Cement and Concrete Association, London 1965, pp. 82-92.